Identification of translocation inhibitors targeting the type III secretion system of enteropathogenic *Escherichia coli*

Sabrina Mühlen[a,b,c], Viktor A. Zapol'skii[d], Ursula Bilitewski[e], Petra Dersch[a,b,c]*

[a] Institute for Infectiology, University of Münster, Münster, Germany

[b] Department of Molecular Infection Biology, Helmholtz Centre for Infection Research, Braunschweig, Germany

[c] German Center for Infection Research (DZIF), Partner site HZI Braunschweig and associated site University of Münster, Germany

[d] Institute of Organic Chemistry, Clausthal University of Technology, Clausthal-Zellerfeld, Germany

[e] Compound Profiling und Screening, Helmholtz Centre for Infection Research, Braunschweig, Germany

* Corresponding author

e-mail: petra.dersch@uni-muenster.de

Running title: Translocation inhibitors of the EPEC T3SS

ABSTRACT

Infections with enteropathogenic *E. coli* (EPEC) cause severe diarrhea in children. The non-invasive bacteria adhere to enterocytes of the small intestine and use a type III secretion system (T3SS) to inject effector proteins into host cells to modify and exploit cellular processes in favor of bacterial survival and replication. Several studies have shown that the T3SSs of bacterial pathogens are essential for virulence. Furthermore, the loss of T3SS-mediated effector translocation results in increased immune recognition and clearance of the bacteria. The T3SS is, therefore, considered a promising target for antivirulence strategies and novel therapeutics development. Here, we report the results of a high-throughput screening assay based on the translocation of the EPEC effector protein Tir. Using this assay, we screened more than 13,000 small molecular compounds of six different compound libraries and identified three substances which showed a significant dose-dependent effect on translocation without adverse effects on bacterial or eukaryotic cell viability. Additionally, these substances reduced bacterial binding to host cells, effector-dependent cell detachment and abolished A/E lesion formation without affecting the expression of components of the T3SS or associated effector proteins. Moreover, no effects of the inhibitors on bacterial motility or Shiga-toxin expression were observed. In summary, we have identified three new compounds that strongly inhibit T3SS-mediated translocation of effectors into mammalian cells, which could be valuable as lead substances for treating EPEC and EHEC infections.

Keywords: EHEC, EPEC, T3SS, virulence inhibitors, small molecule inhibitors, antivirulence strategy

INTRODUCTION

Infection with enteropathogenic *Escherichia coli* (EPEC) is a major cause of infantile diarrhea in children in developing countries (1). EPEC is a member of the family of attaching and effacing (A/E) pathogens, which also includes enterohaemorrhagic *E. coli* (EHEC) and the mouse pathogen *Citrobacter rodentium*. The bacteria in this family intimately adhere to the surface of enterocytes by inducing the formation of characteristic actin-rich pedestals (attachment) and the loss of microvilli (effacement) (2). Subversion of the host actin signaling is mediated by the injection of bacterial effector proteins via a type III secretion system (T3SS). Both, the components of the T3SS, as well as effectors involved in A/E lesion formation, are encoded on the locus of enterocyte effacement pathogenicity island (LEE) located in the bacterial genome (3, 4).

The T3SS of EPEC consists of the basal body, needle, filament and translocon pore (5). The needle is formed by multiple copies of EscF, which form a hollow tube (6) essential for T3S and thus for virulence (7). It is associated on one end with the basal body that powers the translocation and on the other end with a filament made of EspA multimers (6). Together, needle and filament form a channel that upon host cell contact connects the bacterial cytosol with the host cell membrane and initiates the formation of the translocation pore. The translocon pore is formed by heterooligomers of EspB and EspD subunits that are translocated through the channel to the top of which they bind. This complex then inserts into the host cell membrane to form the pore for effector translocation (8). In addition to the T3SS, most translocated effector proteins that are

essential for intimate attachment and pathogenesis are located on the LEE. The translocated intimin receptor (Tir) is the most important and best-studied effector protein of EPEC. After translocation, it inserts into the host cell membrane and acts as a receptor for the bacterial outer membrane protein intimin (9, 10). EPEC strains with a non-functional secretion system, such as Δ*escN* and Δ*espA* mutants, are unable to intimately adhere to enterocytes and were shown to be avirulent in infection models (7).

T3SSs are highly conserved and shared by more than 25 human, plant and zoonotic Gram-negative pathogens (11). Loss of a functional T3SS was also linked with avirulence in the human enteric pathogens *Salmonella*, *Yersinia* and *Shigella* sp. (11). High conservation among the structural components of the T3SSs (11) makes it likely that inhibitors may be found that target the T3SS of more than one bacterial pathogen. Additionally, off-target effects of inhibitors against the T3SS, such as destruction of protective members of the microbiota should be rare, given as T3SSs are only found in pathogenic bacteria. Additionally, the development of resistance mutations to cope with the stresses produced by an inhibitor of the T3SS is less likely as such a substance does not affect bacterial viability or structural integrity (12).

A growing number of studies have identified promising inhibitory compounds that target the T3SS of pathogenic bacteria (13-17). While several, such as Aurodox (18), were shown to be selective in inhibiting the T3SS of only one genus, other compounds, including the salicylidene acylhydrazides showed a broader specificity (19-22). Furthermore, some compounds targeted not only the T3SSs but also bacterial motility (23, 24), suggesting that they affect a conserved target in the basal structure shared between virulence-associated T3SSs and the flagellar export system (25).

Here, we used a high throughput screen to identify substances that inhibit T3S-mediated Tir-effector translocation from EPEC into eukaryotic cells. We identified three promising substances which were able to inhibit Tir translocation into host cells without adverse effects on bacterial or eukaryotic cell viability. We were able to show that the inhibitors interfered with intimate bacterial attachment as well as T3SS-dependent cell detachment in response to infection with an EPEC Δ*espZ* mutant. Inhibitors did not affect the amount of LEE-encoded protein expression or motility.

RESULTS

Screening of natural and chemical compound libraries identified substances that interfere with effector translocation. Translocation of the EPEC effector protein Tir into the host cell was monitored using an EPEC E2348/69 strain expressing a Tir-β-lactamase (TEM) fusion protein encoded under the native promoter in the EPEC genome (26) and the β-lactamase FRET substrate CCF4-AM, which contains the coumarin- and fluorescein-conjugated β-lactam cephalosporin and is green fluorescent. Using a 96-well plate setup, cells were seeded and subsequently infected with EPEC E2348/69 wildtype or E2346/69 P_{LEE5}*tir-blaM.* The bacteria were first grown in T3SS-inducing conditions for two hours and then preincubated in the presence of the screening substances (see **Table 1** for concentrations) for one hour before infection. If translocated into the host cells, the β-lactamase cleaves the CCF4-AM substrate, changing its fluorescence signal from green to blue, which can be quantified in a microtiter plate reader (**Figure 1A**).

Using this assay, we screened two natural and four chemical compound libraries with a total of 13,360 substances (**Table 1, S1**). The z'-values ranged between 0.5 and 0.94 with an average z'-value of 0.76 and an average standard to noise ratio (S/N) of 31.8. Of the tested substances, 50 reduced translocation efficiency by 50 to 75%, while 27 were able to reduce the translocation efficiency of Tir-TEM by more than 75% compared to the control (translocation by untreated E2346/69 P_{LEE5}*tir-blaM*). 24 compounds showed a reduction of 100% (**Figure 1B, Figure S1, Table S1**). These commonly corresponded to known or published antimicrobial substances including chloramphenicol and rifampicin, thuggacin (27-29), tartrolon (30, 31) as well as derivatives of myxovirescin (32), myxovalargin (33, 34) and sorangicin (35). In total, 45 of the primary hit compounds were identified as antimicrobials or compounds with structural homology to known antibiotics, and were thus excluded from further analyses.

Effects of primary hit substances on bacterial growth and cell viability. The remaining 56 inhibitory substances identified in the primary translocation screen were then tested for their dose-dependent effect on bacterial growth behavior. For this, over-night cultures of E2348/69 wildtype were diluted to an OD_{600} of 0.02 and grown in the presence of increasing concentrations of each substance (2.5 µM – 50 µM) at 37°C without shaking for eight hours. At regular intervals (every two hours), the optical density of each sample was measured. Of the 56 compounds retested in dose-response assays, only 35 were confirmed to inhibit translocation. Eight of these substances showed an antibacterial effect, reducing the growth of EPEC E2348/69 by >75% at the highest tested concentration (50 µM) (**Figure 1B**).

To further determine whether the inhibitory substances themselves had any effect on the health of the eukaryotic cells (HEp-2), these were seeded in the presence of the substances and incubated at 37°C with 5% CO_2 for three days. Subsequently, the cell viability was determined by XTT assay. Here, 23 of the tested substances showed marked effects on cellular viability of which two were also shown to have antibiotic activity (**Figure 1B**). In summary, of all tested substances that were neither antimicrobial nor cytotoxic to eukaryotic cells, only six were able to inhibit translocation repeatedly.

Dose-response assays confirmed three substances that inhibit effector translocation without cytotoxicity to eukaryotic cells or EPEC. The six substances, which were able to inhibit T3SS-mediated translocation of the Tir-TEM fusion repeatedly, were purchased or acquired from their respective sources to allow for further analyses. Repetition of the growth, cell viability and translocation assays with the freshly prepared substances demonstrated that three substances (S3 and S4 from SPECS and S6 from the Var library) robustly inhibited Tir-TEM translocation in a dose-dependent manner (**Figure 2A**) with no adverse effects on bacterial or eukaryotic cell viability (**Figure S2**), with their ID_{50} values given in **Table 2**.

To ensure that the observed inhibition of translocation is not due to an effect on the host cells, preventing host-pathogen interaction, HEp-2 cells were pre-treated with the compounds prior to infection. As shown in **Figure S3**, no inhibition of Tir-TEM translocation was observed.

159 The chemical structures of the three identified substances are shown in **Figure 2B**.
160 The substances can be categorized as follows: S3 is a 1,2,4-triazine-5-one, S4 is a p-
161 methoxy-hydrocinnamamide, and substance S6 is a 3-chloroquinoxalin-2(*1H*)-one 4-
162 oxide.
163
164 **Intimate attachment of EPEC to eukaryotic cells was impaired in the presence of**
165 **compounds.** T3SS-mediated translocation of Tir is followed by its integration into the
166 host cell membrane and interaction with the bacterial outer membrane protein intimin.
167 This induces a phosphorylation cascade that results in the accumulation of F-actin
168 underneath the adherent bacteria and the formation of actin-rich pedestals upon which
169 the bacteria reside (2). HEp-2 cells seeded one day before infection were infected with
170 fluorescently-labelled EPEC strain E2348/69 as described for the translocation assay.
171 Cells were fixed after 1.5 hours of infection, and actin pedestals were visualized by
172 fluorescent actin staining (FAS) using phalloidin. While cells infected with wildtype
173 EPEC in the presence of DMSO (negative control) showed the characteristic actin
174 aggregation where bacteria were attached to the cells, no microcolonies or pedestals
175 could be observed in cells treated with either of the compounds (**Figure 3, Figure S4**).
176 In the presence of the compounds, the majority of the bacteria still visible on the cells
177 were not intimately attached to the surface of the cells, no pedestals were formed
178 (**Figure 3**). No obvious differences were observed between the different compounds.
179 This confirmed previous results showing that all three substances blocked Tir
180 translocation, a prerequisite for pedestal formation.
181

Substances inhibited translocation-dependent cell detachment. In a previous study, Berger *et al*. identified EspZ as essential for regulating T3SS-dependent protein translocation (36). They showed that a Δ*espZ* mutant induced cell detachment and cell death due to uncontrolled high effector translocation into host cells (36). Here, we used infection of HeLa cells with an EPEC E2348/69 Δ*espZ* mutant in the presence of inhibitors or DMSO to assess whether the inhibitors could block uncontrolled translocation of effector proteins into the host cell and thus inhibit the described cell detachment phenotype. While infection of HeLa cells with wildtype EPEC or the T3SS mutant Δ*escN* had little effect on cell loss, only approximately 15% of cells remained attached after infection with the Δ*espZ* mutant in the presence of DMSO (**Figure 4A and B**). Interestingly, while cell detachment was inhibited in the presence of inhibitors 50 µM S4 or 25 µM S6, which had an average of ~98% and ~108% of adherent cells compared to uninfected, 50 µM S3 had a less significant effect on cell loss compared to DMSO-treated cells, with ~75% of cells remaining after infection (**Figure 4A and B, Figure S5**).

Expression of LEE-encoded proteins remained unaffected in the presence of the inhibitory compounds. The observed effect of the inhibitors on T3SS-mediated translocation of effector proteins such as Tir may be due to a direct effect on the function of the T3S machinery or an indirect inhibition of the process. An indirect effect could reduce the amount of LEE-proteins (either structural components of the T3SS system or translocated effector proteins) expressed in the presence of the substances. To determine whether such an effect on protein expression could be detected, bacteria

were grown under T3S-inducing conditions in the presence of the inhibitors, and bacterial cell lysates were assessed by immunoblotting. As can be seen in **Figure 5**, the expression levels of the structural components EspA, EspB and EspD as well as the effector protein Tir (fused to β-lactamase as described above) were comparable in inhibitor-treated bacteria and the DMSO-treated negative control (-) (**Figure 5**). This indicated that either the assembly or the export-translocation function of the effectors of the T3S machinery is inhibited by the compounds.

The hemolytic activity of EPEC is affected differently by the different inhibitors. T3SS-dependent hemolysis of sheep red blood cells (RBCs) was described for EPEC (37) and has been attributed to the formation of the T3SS translocon pore in the erythrocyte membrane (8). In a previous study, Kimura *et al.* used this phenotype in their high-throughput screen, which identified Aurodox (18). Here, RBCs were infected with EPEC wildtype in the presence or absence of inhibitors and hemolysis was determined after two hours. A Δ*escN* mutant was used as a control for the T3SS-mediated effect, uninfected RBCs were used as a negative, and saponin-treated cells as a positive control. S3 had no effect on hemolysis, while S4 and S6 significant inhibited hemolysis by ~20% and ~10%, respectively, compared to DMSO-treated cells (**Figure 6**). This indicated that S3 does not seem to interfere with the assembly and translocon pore formation by the T3SS system.

Compounds showed no effect on bacterial motility. Due to the high homology between the basal bodies of the T3SS and flagella (25), a possible effect of the

identified compounds on bacterial motility was investigated. Bacterial motility assays were conducted using LB and DMEM soft agar plates supplemented with 50 µM of each substance. As the motility diameter indicates (**Figure 7**), bacteria were more motile on LB plates (~15 mm) compared to on DMEM plates (~4 mm). Nevertheless, none of the investigated compounds affected bacterial motility when compared to the negative control (DMSO; **Figure 7**). Bacterial growth in both LB and DMEM was confirmed to be unaffected under the respective conditions (**Figure S6**).

Inhibitory substances did not induce Shiga toxin production in reporter-gene assays. Previous results of this study suggest that S3, S4 and S6 are effective compounds suppressing the translocation of crucial virulence factors by the T3SS expressed by EPEC but also by EHEC. This could make them to promising candidates for the treatment or the prevention of bloody diarrhea and the development of hemolytic-uremic syndrome (HUS) in infected patients (38, 39), which is associated with the expression of the Shiga toxin (Stx) by EHEC. As many antimicrobial compounds, that induce DNA damage also induce the expression of the Shiga toxin genes (*stx*) which are encoded on a lambdoid prophage, we wanted to ensure that the induction of toxin expression in response to the identified inhibitors can be excluded. To test this, Shiga toxin expression was assessed using *Gaussia* luciferase reporter gene assays in both, *E. coli* K12 (C600) and *Citrobacter rodentium* (DBS100) strains encoding the *Gaussia* luciferase gene (*Gluc*) under the control of the respective *stx2* promoters (40). Ciprofloxacin, a potent inducer of Shiga toxin expression, was used as a positive control. At their tested maximum concentrations, none of the tested inhibitors induced

reporter-gene expression in *E. coli* K-12 ϕ*stx2*$_a$*::Gluc* (**Figure 8A**) or *C. rodentium* ϕ*stx2*$_{dact}$*::Gluc* (**Figure 8B**) compared to DMSO treated control samples. As expected, reporter strains treated with ciprofloxacin showed strong induction of luciferase expression (**Figure 8A and B**). Therefore, it can be concluded that neither of the inhibitors affects Shiga toxin expression, making them safe not only for the treatment of EPEC infections but also as potential drugs against infections with EHEC.

DISCUSSION

The dramatic increase in antibiotic resistance in recent years has led to a shift in anti-bacterial strategies towards more focused antivirulence-targeted approaches. Interference with virulence mechanisms instead of bacterial survival is promising to reduce the necessity for resistance development as bacteria will only be impaired in their colonization or pathogenicity but able to survive. With no effect on cell survival, the development of resistance mutations or the necessity for uptake of resistance genes is greatly reduced. Anti-virulence strategies have targeted different virulence factors and virulence-associated processes including motility, adhesion and invasion, effector secretion and inter-bacterial signaling (quorum sensing) (12, 16, 17, 22, 41, 42).

Bacterial secretion systems, especially type III and IV secretion systems, are strongly associated with bacterial virulence, as they are used to inject bacterial effectors into the host cells to modulate disease. The loss of functional secretion systems has, therefore, been associated with a loss of pathogenicity of the respective bacteria, rendering pathogens virtually harmless (11). The phenotypes that are associated with functional T3SSs

are diverse. Pathogenic *E. coli* translocate several effector proteins involved in the intimate attachment of the bacteria to the cell surface to withstand being washed off during diarrhea. Other effector proteins mediate the loss of cell-cell junction integrity to invade lower tissues. Furthermore, several effector proteins are involved in the inhibition of innate immune signaling pathways, resulting in the inhibition of cytokine and chemokine release which, in turn, interferes with the recruitment of and clearance by immune cells (43, 44). The formation of the T3SS has also been associated with the formation of pores in and subsequent hemolysis of erythrocytes (8, 37). Moreover, aberrant translocation due to the loss of effectors which control the amount of effector translocation will lead to cell death and detachment (36).

Here, we monitored effector translocation assays in a primary screen to identify small molecule inhibitors that interfere with this process. A Tir-β-lactamase (TEM)-expressing EPEC strain has been used before to study the dynamics of effector translocation in this pathogen (26). Furthermore, this TEM-based assay is commonly used to either screen or confirm identified inhibitory compounds not only in enteropathogenic *E. coli* but also in other T3SS or T4SS-containing pathogens. It has been used to identify or characterize secretion system inhibitors of *Salmonella* (SipB, (23)), *Pseudomonas aeruginosa* (ExoS, (45)) and *Yersinia* (YopE, (46); YopB, (47)), but has also been employed for the T4SSs of *Helicobacter pylori* (48) and *Coxiella burnetii* (49). On the other hand, T3SS-mediated hemolysis was employed as a primary screen in the study, which initially identified the LEE-inhibitor Aurodox (18), while subversion of the host NF-κB inflammatory signaling pathway has been assessed in a study which aimed to

identify inhibitors of the *Yersinia* T3SS and identified the inhibitory substance Piericidin A (50).

In our study setup, bacteria were first grown in T3SS-inducing conditions for two hours before exposing them to the inhibitory substances with which they were incubated for an additional hour. Therefore, the inhibitors that were identified in this screen are unlikely to affect the induction of T3SS-gene expression and injectisome formation as after two hours at T3SS-inducing conditions, the T3SSs have already formed. This hypothesis is supported by the fact that the expression of components of the T3SS as well the Tir-TEM fusion protein is unaffected in the presence of the inhibitors (**Figure 5**). All identified T3SS inhibitors S3, S4 and S6 reduced Tir-TEM translocation, effector-dependent cell detachment and A/E lesion formation to a similar extent/in a comparable manner. Most likely, Tir integration into the host cell membrane is impaired as no translocation into the host cell cytosol could be observed for the Tir-TEM fusion protein (**Figures 2, S2**). Furthermore, the absence of pedestals in the presence of the inhibitors conclusively indicated that no intimate interaction occurred between the bacterial outer membrane protein intimin and its receptor, Tir (**Figures 3 and S4**) (9, 10). In contrast, T3SS-mediated hemolysis of erythrocytes was only inhibited by S4 and S6, but not by S3. The inhibitory effect of S3 appears to be at the translocation/effector level and does not seem to interfere with T3SS assembly as this inhibitor was unable to inhibit hemolysis of erythrocytes (**Figure 6**). As hemolysis is a consequence of T3 translocon pore formation in the erythrocyte membrane, which is dependent on the translocon pore components EspB and EspD (8, 37), it is possible that S4 and S6 affect translocation of all effectors (including the translocation of EspB and EspD) or that they affect translocon

pore-formation *per se* (**Figure 6**). Interestingly, pre-exposure of HEp-2 cells to these inhibitors did not alter the translocation of Tir-TEM by EPEC (**Figure S3**), suggesting that S3, S4 and S6 do not act by influencing host cells. It is likely, that they interfere with the assembly or the function of the T3S apparatus, and it will be interesting to determine the exact mechanism of action of these compounds in future studies.

All three identified inhibitors do not belong to the previously identified classes of T3SS inhibitors. As opposed to previously described T3SS inhibitors (13-17), the inhibitors identified in this study are more specific against the function of the T3SS than previously identified inhibitors. Earlier screens commonly identified inhibitors that affect either gene expression (Aurodox, (51), cytosporone B (52), benzimidazoles (53), sulfonyl amino benzanilides (54), quinolines (55) and salicylidene anilides (24)) or bacterial metabolism (salicylidene acylhydrazides (16), omeprazole ATPase inhibitors (56-58)). While a selective inhibition of LEE (virulence) gene expression is also desirable, inhibitors that affect bacterial metabolism may also result in rapid resistance formation and may also influence the microbiota composition. An effect on the bacterial respiratory chain, which would decrease the formation of the T3SS and thus translocation of effectors was also ruled out for the compounds S3, S4 and S6 identified in this study, as a short-term treatment of bacteria with these inhibitors did not result in significant ATP release (**Figure S7**).

Considering that the identified inhibitors did not affect the expression of the proteins that make up the T3SS or the translocated effector Tir (**Figure 5**), we tested the effect of the inhibitors on the translocation of other effector proteins into the host cell by making use of known effector deletion mutants and their associated phenotypes.

342 Deletion of the gene for the LEE-encoded effector protein EspZ results in aberrant
343 effector translocation into host cells, resulting in host cell detachment due to cell death
344 (36). Preincubation of bacteria in the presence of the inhibitors efficiently reduced cell
345 detachment compared to the positive control (Δ*espZ* + DMSO), suggesting that effector
346 translocation into the host cells was indeed impaired (**Figures 4 and S5**).

347 The homologies between the basal body of the T3SS and the bacterial flagellar basal
348 body are commonly appreciated (25). While an inhibitory effect on bacterial motility
349 would not be undesirable, no effect of any of the newly described substances could be
350 observed (**Figure 7**). This, too, supports the hypothesis that the inhibitors do not
351 interfere with conserved basal body structures of the T3SS, but rather with the
352 assembly of the injectisome or the translocation of the effector proteins. Also, other
353 compounds have been identified that interfere with T3SS function, e.g. (-)-hopeaphenol
354 which seem to localize on the outer membrane and interfere with the closely related
355 T3S apparatus of *Yersinia pseudotuberculosis*, *Pseudomonas aeruginosa* and
356 *Chlamydia trachomatis* (59), and thiazolidinone derivatives that inhibit T3SS in *S.*
357 *enterica* serovar Typhimurium, *Pseudomonas syringae* and *Francisella tularensis* most
358 likely by targeting the outer membrane secretin component of the T3SS (60). In
359 addition, a picolinic acid derivative and a symmetric dipropionate were found to be
360 active against effector secretion of *Y. pestis* without cytotoxicity against mammalian
361 cells, and notably, they were also active against the translocated intimin receptor Tir in
362 EPEC (46). As their molecular targets are also still unknown, it would be interesting to
363 investigate whether they inhibit identical T3SS functions as the identified compounds
364 S3, S4 or S6.

The effective blockage of T3SS expressed by EPEC as well as by frequent EHEC strains makes the identified inhibitors promising candidates for therapies against hemorrhagic uremic syndrome, which is not curable by common antibiotics such as ciprofloxacin which induce the Shiga toxin genes encoded on lysogenic phages within the bacterial genome (61, 62). As all three inhibitory substances showed no inducing effect on Shiga toxin reporter-gene expression (**Figure 8**), they most likely do not induce/enhance disease progression to HUS. Furthermore, we discovered that even 5-fold excess concentrations (250 µM) of the inhibitors did not affect bacterial growth in MIC studies (**Figure S8**), providing further promise that resistance development against these inhibitory substances may be slow as little selective pressure is induced.

Taken together, our study revealed three potent small molecule inhibitors blocking T3SS-mediated translocation of crucial virulence factors of EPEC/EHEC. As all three compounds interfere with the infection at later stages, e. g. after the T3SS has formed, they constitute promising drugs for therapeutic treatment of the infection, as T3SS-formation will have already occurred once treatment commences.

Materials and Methods

Bacterial strains and cell lines. Bacterial strains (listed in **Table S2**) were grown in Luria Bertani (LB; Carl Roth, Germany) or Müller-Hinton (MH; Sigma Aldrich, Germany) broth or DMEM GlutaMAX (Gibco) as indicated. LB overnight cultures were supplemented with antibiotics tetracycline (30 µg/ml), carbenicillin (100 µg/ml) or kanamycin (50 µg/ml) for selection where required.

Cell lines and their respective growth media are given in **Table S3**. Eukaryotic cells were cultured at 37°C, 5% CO_2.

Infection of eukaryotic cells. One day before infection, bacteria were inoculated into LB broth and grown at 37°C and 180 rpm overnight. On the day of infection, overnight cultures were diluted 1:75 in DMEM GlutaMAX (Gibco) and grown statically for three hours at 37°C with 5% CO_2.

HEp-2 cells were washed twice with Dulbecco's PBS (DPBS; Sigma) and infected with EPEC grown to an $OD_{600\ nm}$ of 0.03 for three hours.

Small molecule compound libraries

All used two natural and four chemical libraries are given in **Table 1** with concentration of stock solutions and sources.

Effector translocation assay. For translocation assays, $2x10^5$ HEp-2 (ATCC CCL-23) cells/ml were seeded into black 96-well plates with transparent bottom (Costar, Germany). Bacterial overnight cultures were diluted 1:50 into an appropriate amount of DMEM with GlutaMAX (Gibco, Germany) and incubated for two hours at 37°C 5% CO_2. 2.5 mM probenecid were added to the cultures which were diluted 1:2 in DMEM with GlutaMAX (Gibco, Germany). 50 µl of the bacterial suspension were subsequently added to the screening plates which contained 1 µl of compound per well (concentrations are given in **Table 1**). These plates were incubated for an additional hour. HEp-2 cells were washed once with Dulbecco's PBS (DPBS; Sigma, Germany)

and 50 µl DMEM with GlutaMAX was added to each well. The bacteria-inhibitor suspension (50 µl per well) was then added to the cells, the plates were centrifuged at 1,000 x g for one minute (Eppendorf Centrifuge 5810R with a A-2-DWP-AT plate rotor) and incubated for 1.5 hours (37°C, 5% CO_2). Media was then removed, and infected cells were washed twice with DPBS. DMEM with GlutaMAX supplemented with 1 mM HEPES (Biochrom, Germany) and 1x gentamicin (Sigma) was added to the cells and mixed with LifeBLAzer CCF4-AM staining solution (Invitrogen). The plates were then incubated for one hour at room temperature. Subsequently, the fluorescence was determined in a VarioSkan (Fisher Scientific, Germany) or ClarioStar Plus (BMG Labtech, Germany) plate reader using an excitation wavelength of 405 nm (10 nm bandwidth). Emission was detected with 460 nm (20 nm bandwidth, blue fluorescence) and 530 nm (15 nm bandwidth, green fluorescence) filters. Effector translocation was determined by calculating the ratio of blue to green fluorescence ($Em_{520\ nm}$/ $Em_{460\ nm}$). The translocation efficiency of untreated, EPEC-infected cells was set to 100% while that of untreated EPEC-infected cells was used as a negative control.

Analysis of inhibitors on *in vitro* growth and cell viability. Wildtype EPEC E2348/69 was grown overnight in LB at 37°C and resuspended to an optical density (OD_{600nm}) of 0.02. 100 µl were added to each well of a 96-well plate containing appropriate amounts of substance or control. Plates were incubated at 37°C without shaking and the OD_{600nm} was determined every two hours for eight hours in a VarioSkan (Fisher Scientific, Germany) or ClarioStar Plus (BMG Labtech, Germany) plate reader.

To determine the effect of inhibitory substances on the viability of eukaryotic cells, 100 µl of a $2x10^4$ cells/ml solution was used to resuspend the inhibitors of interest, and the resulting solution was transferred to a tissue culture treated 96-well plate. Plates were incubated at 37°C, 5% CO_2 for three days. Subsequently, media was aspirated, and a solution of XTT/PMS (Cell Proliferation Kit II; Merck, Germany) and culture medium was added to the wells. Cells were then incubated at 37°C 5% CO_2 for an additional two hours after which cell viability was determined at 475 nm in a VarioSkan (Fisher Scientific, Germany) or ClarioStar Plus (BMG Labtech, Germany) plate reader.

Fluorescent actin stain (FAS). Cells seeded on coverslips at $2x10^5$ cells/ml were infected as described above. After infection, cells were washed twice with DPBS, fixed with 4% paraformaldehyde (Sigma, Germany) for 20 min and permeabilized with 0.1% Triton X-100 (OMNI Life Science, Germany) for five minutes at RT. After washing, cells were stained with TRITC-Phalloidin (Sigma Aldrich, Germany), washed again and mounted using Prolong Diamond mounting medium containing DAPI (Thermo Fisher Scientific, Germany). Actin pedestals on cells were visualized using a Keyence Biorevo BZ-9000 (Keyence, Germany).

Cell detachment assay. Cell detachment assays were carried out, as described in (36). In short, HeLa cells were seeded 48 hours prior to infection with EPEC primed in the presence or absence of inhibitors. After one hour of infection, cells were washed five times with DPBS, incubated in the presence of inhibitors for an additional hour and washed again five times with DPBS. Cells were trypsinized and counted in a

455 hemocytometer to determine the percentage of remaining cells. For visualization, HeLa
456 cells grown in 8-well removable cell culture chambers (Sarstedt, Germany) or on
457 coverslips were infected and treated as described above. Following the second washing
458 step, cells were fixed with 4% PFA and subsequently stained using the Hematoxylin-
459 Eosin fast staining kit (Carl Roth, Germany) according to (36).
460
461 **Motility assay.** LB and DMEM motility agar plates (0.3% agar) containing inhibitory
462 substances at a concentration of 50 µM/ml were stab-inoculated using 2 µl of an EPEC
463 E2348/69 overnight culture and incubated at 37°C overnight. The diameter of the
464 motility halos was documented after 6 (LB) or 24 (DMEM) hours. Triplicate stabs were
465 done per assay for each inhibitor.
466
467 **Protein expression and extraction.** For analysis of effector protein expression, LB
468 overnight cultures of bacteria were diluted 1:50 into DMEM GlutaMAX in the presence
469 or absence of inhibitors. After stationary incubation of the cultures at 37°C, 5% CO_2 for
470 three hours, equalized amounts of cells were harvested by centrifugation at 8,000 x g
471 for 10 minutes. The supernatants were discarded, and the bacterial pellets were
472 resuspended in BugBuster protein extraction reagent (Merck, Germany). The cell
473 suspensions were incubated on a rotary shaker for 20 minutes. SDS sample buffer was
474 added before the samples were boiled at 95°C for 10 minutes before further analysis.
475
476 **SDS-PAGE and immunoblotting.** 12% SDS-polyacrylamide gels were used to
477 separate proteins with the BioRad MiniPROTEAN Electrophoresis System (BioRad,

Germany) followed by transfer of the proteins onto Immobilon FL PVDF membrane (Millipore, Germany). Antibodies against the T3SS components EspA (1:500), EspB (1:10,000) and EspD (1:10,000) (63) and anti-β-lactamase antibody (Abcam; 1:5,000) against the Tir-β-lactamase fusion protein were used to detect protein by immunoblotting. GAPDH (MA5-15738; 1:5,000; ThermoFisherScientific, Germany) was used as a loading control. Using anti-mouse IgG HRP-linked secondary antibody (Cell Signaling Technology, Germany), proteins were detected with WesternLightning ECL Reagent (Perkin Elmer, Germany) and exposure of the membrane to CL-XPosure film (ThermoFisher Scientific, Germany).

Hemolysis assay. EPEC overnight cultures were diluted 1:25 in DMEM high glucose without Phenol Red (Sigma, Germany) and grown for three hours at 37°C, 5% CO_2 in the presence or absence of inhibitors. Sheep RBCs in Alsever (Fiebig Nährstofftechnik, Germany) were washed three times in PBS and resuspended to 5% (vol/vol) in DMEM high glucose without Phenol Red (Sigma, Germany). Bacterial cultures were equalized to $1x10^8$ in 500 µl and added to 500 µl sheep RBCs (5% vol/vol) in two ml Eppendorf tubes. Uninfected RBCs in DMEM were used as a negative control. Total lysis was achieved by the addition of 0.2% saponin to the culture medium. To synchronize infection and mediate bacterial-cell contact, tubes were centrifuged one minute at 2,500 x *g* (Eppendorf MiniSpin) before incubation at 37°C, 5% CO_2. After two hours, cells were gently resuspended, followed by centrifugation at 2,500 x g for one minute. 100 µl of each supernatant was transferred to a 96-well plate, and the amount of hemoglobin released was assessed at 543 nm in a ClarioStar Plus plate reader (BMG Labtech,

Germany). Hemolysis was calculated as the percentage of hemoglobin released by the DMSO-treated wildtype-infected RBCs.

Reporter-gene assays. C600 (*stx2*::*Gluc*) and DBS100 (*stx2*$_{dact}$::*Gluc*). Bacteria were inoculated into LB broth and grown at 37°C, 200 rpm for 16 hours in the presence of either the inhibitors at their highest non-cytotoxic concentration, DMSO (negative control; AppliChem) or 40 ng/ml ciprofloxacin (positive control; Sigma). The optical density of each culture was determined, and a volume corresponding to an OD_{600nm} of one (10^9 cells) was pelleted at 14,000 x *g* for one minute (Eppendorf MiniSpin). 20 µl of supernatant was mixed with 50 µl BioLux *Gaussia* Luciferase Assay substrate (New England Biolabs, Germany) and the luciferase activity was determined in a ClarioStar Plus plate reader (BMG Labtech, Germany) according to the manufacturer's recommendations. Values were compared to untreated culture supernatant, and LB medium was used as blank.

Acknowledgements

We thank Ilan Rosenshine for kindly providing the E2348/69 P_{LEE5}*tir-blaM* strain and Martin Koeppel and Bärbel Stecher for the use of C600 ϕ*stx2*$_a$::*Gluc* and DBS770 ϕ*stx2*$_{dact}$*::Gluc*. We also thank Sandra Stengel and Amrei Rolof for technical assistance with the HTS. Petra Dersch, Ursula Bilitewski and Sabrina Mühlen are supported by the Deutsche Zentrum für Infektionsforschung (DZIF TTU-GI, TTU 06.801-2, TTU_06_819_00).

REFERENCES

1. Nataro JP, Kaper JB. 1998. Diarrheagenic *Escherichia coli*. Clin Microbiol Rev 11:142-201.
2. Frankel G, Phillips AD, Rosenshine I, Dougan G, Kaper JB, Knutton S. 1998. Enteropathogenic and enterohaemorrhagic *Escherichia coli*: more subversive elements. Mol Microbiol 30:911-21.
3. Iguchi A, Thomson NR, Ogura Y, Saunders D, Ooka T, Henderson IR, Harris D, Asadulghani M, Kurokawa K, Dean P, Kenny B, Quail MA, Thurston S, Dougan G, Hayashi T, Parkhill J, Frankel G. 2009. Complete genome sequence and comparative genome analysis of enteropathogenic *Escherichia coli* O127:H6 strain E2348/69. J Bacteriol 191:347-54.
4. McDaniel TK, Jarvis KG, Donnenberg MS, Kaper JB. 1995. A genetic locus of enterocyte effacement conserved among diverse enterobacterial pathogens. Proc Natl Acad Sci U S A 92:1664-8.
5. Gaytan MO, Martinez-Santos VI, Soto E, Gonzalez-Pedrajo B. 2016. Type three secretion system in attaching and effacing pathogens. Front Cell Infect Microbiol 6:129.
6. Wilson RK, Shaw RK, Daniell S, Knutton S, Frankel G. 2001. Role of EscF, a putative needle complex protein, in the type III protein translocation system of enteropathogenic *Escherichia coli*. Cell Microbiol 3:753-62.
7. Deng W, Puente JL, Gruenheid S, Li Y, Vallance BA, Vazquez A, Barba J, Ibarra JA, O'Donnell P, Metalnikov P, Ashman K, Lee S, Goode D, Pawson T, Finlay BB.

2004. Dissecting virulence: systematic and functional analyses of a pathogenicity island. Proc Natl Acad Sci U S A 101:3597-602.

8. Ide T, Laarmann S, Greune L, Schillers H, Oberleithner H, Schmidt MA. 2001. Characterization of translocation pores inserted into plasma membranes by type III-secreted Esp proteins of enteropathogenic *Escherichia coli*. Cell Microbiol 3:669-79.
9. Kenny B, DeVinney R, Stein M, Reinscheid DJ, Frey EA, Finlay BB. 1997. Enteropathogenic *E. coli* (EPEC) transfers its receptor for intimate adherence into mammalian cells. Cell 91:511-20.
10. Hartland EL, Batchelor M, Delahay RM, Hale C, Matthews S, Dougan G, Knutton S, Connerton I, Frankel G. 1999. Binding of intimin from enteropathogenic *Escherichia coli* to Tir and to host cells. Mol Microbiol 32:151-8.
11. Cornelis GR. 2006. The type III secretion injectisome. Nat Rev Microbiol 4:811-25.
12. Muhlen S, Dersch P. 2016. Anti-virulence strategies to target bacterial infections. Curr Top Microbiol Immunol 398:147-183.
13. Charro N, Mota LJ. 2015. Approaches targeting the type III secretion system to treat or prevent bacterial infections. Expert Opin Drug Discov 10:373-87.
14. Duncan MC, Linington RG, Auerbuch V. 2012. Chemical inhibitors of the type three secretion system: disarming bacterial pathogens. Antimicrob Agents Chemother 56:5433-41.
15. Pendergrass HA, May AE. 2019. Natural product type III secretion system inhibitors. Antibiotics (Basel) 8.
16. Zambelloni R, Marquez R, Roe AJ. 2015. Development of antivirulence compounds: a biochemical review. Chem Biol Drug Des 85:43-55.

570 17. McShan AC, De Guzman RN. 2015. The bacterial type III secretion system as a
571 target for developing new antibiotics. Chem Biol Drug Des 85:30-42.
572 18. Kimura K, Iwatsuki M, Nagai T, Matsumoto A, Takahashi Y, Shiomi K, Omura S,
573 Abe A. 2011. A small-molecule inhibitor of the bacterial type III secretion system
574 protects against *in vivo* infection with *Citrobacter rodentium*. J Antibiot (Tokyo)
575 64:197-203.
576 19. Veenendaal AK, Sundin C, Blocker AJ. 2009. Small-molecule type III secretion
577 system inhibitors block assembly of the *Shigella* type III secreton. J Bacteriol
578 191:563-70.
579 20. Wolf K, Betts HJ, Chellas-Gery B, Hower S, Linton CN, Fields KA. 2006. Treatment
580 of *Chlamydia trachomatis* with a small molecule inhibitor of the *Yersinia* type III
581 secretion system disrupts progression of the chlamydial developmental cycle. Mol
582 Microbiol 61:1543-55.
583 21. Izore T, Job V, Dessen A. 2011. Biogenesis, regulation, and targeting of the type III
584 secretion system. Structure 19:603-12.
585 22. Beckham KS, Roe AJ. 2014. From screen to target: insights and approaches for the
586 development of anti-virulence compounds. Front Cell Infect Microbiol 4:139.
587 23. Negrea A, Bjur E, Ygberg SE, Elofsson M, Wolf-Watz H, Rhen M. 2007.
588 Salicylidene acylhydrazides that affect type III protein secretion in *Salmonella*
589 *enterica* serovar typhimurium. Antimicrob Agents Chemother 51:2867-76.
590 24. Kauppi AM, Nordfelth R, Uvell H, Wolf-Watz H, Elofsson M. 2003. Targeting
591 bacterial virulence: inhibitors of type III secretion in *Yersinia*. Chem Biol 10:241-9.

592 25. Diepold A, Armitage JP. 2015. Type III secretion systems: the bacterial flagellum
593 and the injectisome. Philos Trans R Soc Lond B Biol Sci 370.
594 26. Mills E, Baruch K, Charpentier X, Kobi S, Rosenshine I. 2008. Real-time analysis of
595 effector translocation by the type III secretion system of enteropathogenic
596 *Escherichia coli*. Cell Host Microbe 3:104-13.
597 27. Irschik H, Reichenbach H, Hofle G, Jansen R. 2007. The thuggacins, novel
598 antibacterial macrolides from *Sorangium cellulosum* acting against selected Gram-
599 positive bacteria. J Antibiot (Tokyo) 60:733-8.
600 28. Buntin K, Irschik H, Weissman KJ, Luxenburger E, Blocker H, Muller R. 2010.
601 Biosynthesis of thuggacins in myxobacteria: comparative cluster analysis reveals
602 basis for natural product structural diversity. Chem Biol 17:342-56.
603 29. Bock M, Dehn R, Kirschning A. 2008. Total synthesis of thuggacin B. Angew Chem
604 Int Ed Engl 47:9134-7.
605 30. Irschik H, Schummer D, Gerth K, Hofle G, Reichenbach H. 1995. The tartrolons,
606 new boron-containing antibiotics from a myxobacterium, *Sorangium cellulosum*. J
607 Antibiot (Tokyo) 48:26-30.
608 31. Elshahawi SI, Trindade-Silva AE, Hanora A, Han AW, Flores MS, Vizzoni V,
609 Schrago CG, Soares CA, Concepcion GP, Distel DL, Schmidt EW, Haygood MG.
610 2013. Boronated tartrolon antibiotic produced by symbiotic cellulose-degrading
611 bacteria in shipworm gills. Proc Natl Acad Sci U S A 110:E295-304.
612 32. Gerth K, Irschik H, Reichenbach H, Trowitzsch W. 1982. The myxovirescins, a
613 family of antibiotics from *Myxococcus virescens* (Myxobacterales). J Antibiot
614 (Tokyo) 35:1454-9.

615 33. Irschik H, Gerth K, Kemmer T, Steinmetz H, Reichenbach H. 1983. The
616 myxovalargins, new peptide antibiotics from *Myxococcus fulvus* (Myxobacterales). I.
617 Cultivation, isolation, and some chemical and biological properties. J Antibiot
618 (Tokyo) 36:6-12.
619 34. Irschik H, Reichenbach H. 1985. The mechanism of action of myxovalargin A, a
620 peptide antibiotic from *Myxococcus fulvus*. J Antibiot (Tokyo) 38:1237-45.
621 35. Irschik H, Jansen R, Gerth K, Hofle G, Reichenbach H. 1987. The sorangicins,
622 novel and powerful inhibitors of eubacterial RNA polymerase isolated from
623 myxobacteria. J Antibiot (Tokyo) 40:7-13.
624 36. Berger CN, Crepin VF, Baruch K, Mousnier A, Rosenshine I, Frankel G. 2012. EspZ
625 of enteropathogenic and enterohemorrhagic *Escherichia coli* regulates type III
626 secretion system protein translocation. mBio 3.
627 37. Warawa J, Finlay BB, Kenny B. 1999. Type III secretion-dependent hemolytic
628 activity of enteropathogenic *Escherichia coli.* Infect Immun 67:5538-40.
629 38. Karmali MA, Steele BT, Petric M, Lim C. 1983. Sporadic cases of haemolytic-
630 uraemic syndrome associated with faecal cytotoxin and cytotoxin-producing
631 *Escherichia coli* in stools. Lancet 1:619-20.
632 39. O'Brien AD, Lively TA, Chang TW, Gorbach SL. 1983. Purification of Shigella
633 dysenteriae 1 (Shiga)-like toxin from *Escherichia coli* O157:H7 strain associated
634 with haemorrhagic colitis. Lancet 2:573.
635 40. Muhlen S, Ramming I, Pils MC, Koeppel M, Glaser J, Leong J, Flieger A, Stecher B,
636 Dersch P. 2020. Identification of antibiotics that diminish disease in a murine model

637 of enterohemorrhagic *Escherichia coli* infection. Antimicrob Agents Chemother
638 doi:10.1128/AAC.02159-19.
639 41. Escaich S. 2008. Antivirulence as a new antibacterial approach for chemotherapy.
640 Curr Opin Chem Biol 12:400-8.
641 42. Dickey SW, Cheung GYC, Otto M. 2017. Different drugs for bad bugs: antivirulence
642 strategies in the age of antibiotic resistance. Nat Rev Drug Discov 16:457-471.
643 43. Shenoy AR, Furniss RCD, Goddard PJ, Clements A. 2018. Modulation of host cell
644 processes by T3SS effectors. Curr Top Microbiol Immunol 416:73-115.
645 44. Riebisch AK, Muhlen S. 2020. Attaching and effacing pathogens: the effector ABC
646 of immune subversion. Future Microbiol 15:945-958.
647 45. Aiello D, Williams JD, Majgier-Baranowska H, Patel I, Peet NP, Huang J, Lory S,
648 Bowlin TL, Moir DT. 2010. Discovery and characterization of inhibitors of
649 *Pseudomonas aeruginosa* type III secretion. Antimicrob Agents Chemother
650 54:1988-99.
651 46. Pan NJ, Brady MJ, Leong JM, Goguen JD. 2009. Targeting type III secretion in
652 *Yersinia pestis*. Antimicrob Agents Chemother 53:385-92.
653 47. Harmon DE, Davis AJ, Castillo C, Mecsas J. 2010. Identification and
654 characterization of small-molecule inhibitors of Yop translocation in *Yersinia*
655 *pseudotuberculosis*. Antimicrob Agents Chemother 54:3241-54.
656 48. Schindele F, Weiss E, Haas R, Fischer W. 2016. Quantitative analysis of CagA type
657 IV secretion by Helicobacter pylori reveals substrate recognition and translocation
658 requirements. Mol Microbiol 100:188-203.

659 49. Newton P, Thomas DR, Reed SCO, Lau N, Xu B, Ong SY, Pasricha S,
660 Madhamshettiwar PB, Edgington-Mitchell LE, Simpson KJ, Roy CR, Newton HJ.
661 2020. Lysosomal degradation products induce *Coxiella burnetii* virulence. Proc Natl
662 Acad Sci U S A 117:6801-6810.
663 50. Duncan MC, Wong WR, Dupzyk AJ, Bray WM, Linington RG, Auerbuch V. 2014. An
664 NF-kappaB-based high-throughput screen identifies piericidins as inhibitors of the
665 *Yersinia pseudotuberculosis* type III secretion system. Antimicrob Agents
666 Chemother 58:1118-26.
667 51. McHugh RE, O'Boyle N, Connolly JPR, Hoskisson PA, Roe AJ. 2019.
668 Characterization of the mode of action of Aurodox, a type III secretion system
669 Inhibitor from *Streptomyces goldiniensis*. Infect Immun 87.
670 52. Li J, Lv C, Sun W, Li Z, Han X, Li Y, Shen Y. 2013. Cytosporone B, an inhibitor of
671 the type III secretion system of *Salmonella enterica* serovar Typhimurium.
672 Antimicrob Agents Chemother 57:2191-8.
673 53. Marsden AE, King JM, Spies MA, Kim OK, Yahr TL. 2016. Inhibition of
674 *Pseudomonas aeruginosa* ExsA DNA-binding activity by N-Hydroxybenzimidazoles.
675 Antimicrob Agents Chemother 60:766-76.
676 54. Gauthier A, Robertson ML, Lowden M, Ibarra JA, Puente JL, Finlay BB. 2005.
677 Transcriptional inhibitor of virulence factors in enteropathogenic *Escherichia coli*.
678 Antimicrob Agents Chemother 49:4101-9.
679 55. Koppolu V, Osaka I, Skredenske JM, Kettle B, Hefty PS, Li J, Egan SM. 2013.
680 Small-molecule inhibitor of the *Shigella flexneri* master virulence regulator VirF.
681 Infect Immun 81:4220-31.

682 56. Case HB, Mattock DS, Dickenson NE. 2018. Shutting down *Shigella* secretion:
683 characterizing small molecule type three secretion system ATPase inhibitors.
684 Biochemistry 57:6906-6916.
685 57. Puiac S, Sem X, Negrea A, Rhen M. 2011. Small-molecular virulence inhibitors
686 show divergent and immunomodulatory effects in infection models of *Salmonella*
687 *enterica* serovar Typhimurium. Int J Antimicrob Agents 38:409-16.
688 58. Layton AN, Hudson DL, Thompson A, Hinton JC, Stevens JM, Galyov EE, Stevens
689 MP. 2010. Salicylidene acylhydrazide-mediated inhibition of type III secretion
690 system-1 in *Salmonella enterica* serovar Typhimurium is associated with iron
691 restriction and can be reversed by free iron. FEMS Microbiol Lett 302:114-22.
692 59. Zetterstrom CE, Hasselgren J, Salin O, Davis RA, Quinn RJ, Sundin C, Elofsson M.
693 2013. The resveratrol tetramer (-)-hopeaphenol inhibits type III secretion in the
694 gram-negative pathogens *Yersinia pseudotuberculosis* and *Pseudomonas*
695 *aeruginosa*. PLoS One 8:e81969.
696 60. Felise HB, Nguyen HV, Pfuetzner RA, Barry KC, Jackson SR, Blanc MP, Bronstein
697 PA, Kline T, Miller SI. 2008. An inhibitor of gram-negative bacterial virulence protein
698 secretion. Cell Host Microbe 4:325-36.
699 61. Kakoullis L, Papachristodoulou E, Chra P, Panos G. 2019. Shiga toxin-induced
700 haemolytic uraemic syndrome and the role of antibiotics: a global overview. J Infect
701 79:75-94.
702 62. Zimmerhackl LB. 2000. E. coli, antibiotics, and the hemolytic-uremic syndrome. N
703 Engl J Med 342:1990-1.

704 63. Beinke C, Laarmann S, Wachter C, Karch H, Greune L, Schmidt MA. 1998.
705 Diffusely adhering *Escherichia coli* strains induce attaching and effacing phenotypes
706 and secrete homologs of Esp proteins. Infect Immun 66:528-39.

707

708

709

TABLES:

Table 1: Screened natural and chemical compound libraries

Compound library	Source	Number of compounds	Stock solution concentration [mM]	Remarks
NCh + ExNCl	HIPS, Univ. Tübingen via DZIF	264 + 352	1 and 10	Microbial secondary metabolites
SPECS	Specs, The Netherlands	2171	10	Chemical synthesis
LOPAC	Sigma	1408	10	Known bioactive compounds
Var	Various research groups	2933	5 or 10	Chemical synthesis
EMC	EMC microcollections GmbH, Tübingen	6232	1	Chemical synthesis

Table 2: IC_{50} values for translocation efficiency of Tir-TEM as determined with GraphPad Prism using a non-linear regression fit, variable slope (four parameters) with 95% confidence interval

Compound	IC_{50} [µM]
S3	± 33.77
S4	± 8.207
S6	± 9.347

720

721 **FIGURE LEGENDS**

722 **FIG 1** Illustration of inhibitor screen setup and screen summary. For the translocation
723 assay, bacteria were grown overnight in LB broth and diluted 1:50 into DMEM. The
724 infection cultures were grown under T3SS-inducing conditions (37°C, 5% CO_2) for two
725 hours and subsequently added to 96-well plates containing one µl of the screen sub-
726 stances per well. The bacteria were incubated for an additional hour in the presence of
727 substances before being added to a 96-well plate containing HEp-2 cells. Infection was
728 synchronized by centrifugation. Cells were infected in the presence of inhibitors for 1.5
729 hours. Bacteria were removed and cells stained with the FRET substrate CCF4-AM for
730 one hour. Translocation efficiency was assessed by measuring blue and green
731 fluorescence (**A**). Of all the libraries screened, compounds that reduced the
732 translocation by more than 50% in the initial screen were further assessed for cytotoxic
733 and antibacterial side-effects. Three inhibitory compounds without adverse effects were
734 used for further analysis (**B**). Figures were created with BioRender.com.

735

736 **FIG 2** Three substances of the initial high-throughput screen inhibit Tir translocation in a
737 dose-dependent manner. Translocation assays were carried out as described for the
738 high throughput screen. The dose-dependent translocation of Tir-TEM in the presence
739 of the three inhibitory substances identified in the high throughput screen was
740 determined with purchased substances. The ratio of blue/green fluorescence was
741 determined, and values are given as mean (± SEM) of two independent experiments.
742 Curves are analyzed in GraphPad Prism using a non-linear regression fit, variable slope

743 (four parameters) with 95% confidence interval (**A**). Chemical structures of the three
744 substances (drawn using ChemDraw) (**B**).
745
746 **FIG 3** Intimate attachment of EPEC is abolished in the presence of inhibitory
747 substances. HEp-2 cells were infected with EPEC strain E2348/69 pP_{gapdh}*amCyan*
748 (green) in the presence of either inhibitory substances or DMSO (control) for 1.5 hours.
749 After rinsing with DPBS, cells were fixed, permeabilized and stained with TRITC-
750 Phalloidin to visualize F-actin (red). Coverslips were mounted with ProLong Diamond
751 mounting medium containing DAPI for staining of DNA (blue). Cells were visualized
752 using a Keyence Biorevo BZ-9000. Scale bars depict 10 µm.
753
754 **FIG 4** Substances inhibit effector-mediated cell loss. Cells were infected with an EPEC
755 E2348/69 Δ*espZ* mutant in the presence of either 50 µM S3 or S4 and 25 µM S6 or an
756 equivalent amount of DMSO for three hours. Cells were thoroughly washed with DPBS
757 five times every hour. The number of adherent cells after infection was determined by
758 trypsinizing remaining cells at the end of the experiment and counting them in a
759 hemocytometer. The number of cells in uninfected, untreated samples was set to 100%.
760 Shown are the mean values (±SEM) of adherent cells determined in three independent
761 experiments performed at least in triplicate. Statistical analysis was performed via
762 Welch's t-test (*, $P < 0.05$; **, $P < 0.01$; ***, $P < 0.001$; ****, $P < 0.0001$), with all treated
763 groups compared to DMSO-treated, Δ*espZ*-infected control cells (**A**). To visualize the
764 amount of cells remaining after three hours, cells were fixed and stained with
765 Hematoxylin Eosin staining solution. Cells were visualized using a Keyence Biorevo BZ-

9000 (**B**). Pictures are representative of three independent experiments conducted in triplicate.

FIG 5 The expression levels of LEE-encoded T3SS proteins are unaffected by the translocation inhibitors. Cell lysates of bacteria grown under T3SS-inducing conditions (37°C, 5% CO_2) for three hours and equalized for cell numbers were separated by SDS-PAGE. The protein expression levels of the proteins EspA, EspB and EspD, which make up the T3SS filament and translocon pore, as well as the level of the Tir-TEM fusion protein were evaluated by immunoblotting. Depicted blots are representative of at least three independent experiments (**A**). The schematic of the T3SS shows the localization of the analyzed components in the T3SS complex. The figure was created with BioRender.com (**B**).

FIG 6 Hemolysis of sheep red blood cells (RBC) was reduced in the presence of S4 and S6 but not by S3. A 3% RBC suspension was incubated with $1x10^8$ bacteria in the presence of either inhibitors or DMSO for two hours. Cells were pelleted, supernatants transferred to 96-well plates, and the amount of hemoglobin released from the cells was determined by measuring absorbance at 543 nm in a plate reader. Shown are the mean values (±SEM) of the percentage of hemolysis inhibition determined in three independent experiments performed in triplicate with all treated groups compared to DMSO-treated, wildtype-infected control cells. Statistical analysis was performed via Welch's t-test (*, $P < 0.05$; **, $P < 0.01$; ***, $P < 0.001$; ****, $P < 0.0001$).

FIG 7 The T3SS inhibiting compounds S3, S4 and S6 do not affect the flagellar T3SS. Bacterial motility was assessed by stab-inoculating bacteria into LB- or DMEM-motility agar containing inhibitors (50 µM S3 or S4, 25 µM S6) or DMSO. After six hours (LB; **A**), 24 hours and 48 hours (DMEM; **B**) the diameters of the motility halo were measured. All assays were carried out three times in triplicate. Differences in diameter in the presence of substances compared to DMSO were not significant. Statistical analysis was performed with Welch's t-test.

FIG 8 The expression of Shiga toxin is unaffected by the inhibitory compounds. *E. coli* (**A**) or *C. rodentium* (**B**) expressing the *Gaussia* luciferase gene (*Gluc*) under the control of the Shiga toxin promoter were grown overnight in the presence of either compounds, DMSO, or Ciprofloxacin (positive control), equalized and the amount of luciferase released into the supernatant was determined by *Gaussia* luciferase assay. Given are the mean RLU values (±SEM) of three independent experiments performed in triplicate. Statistical analysis was performed via Welch's t-test (*, $P < 0.05$; **, $P < 0.01$; ***, $P < 0.001$; ****, $P < 0.0001$), with all treated groups compared to DMSO-treated control.

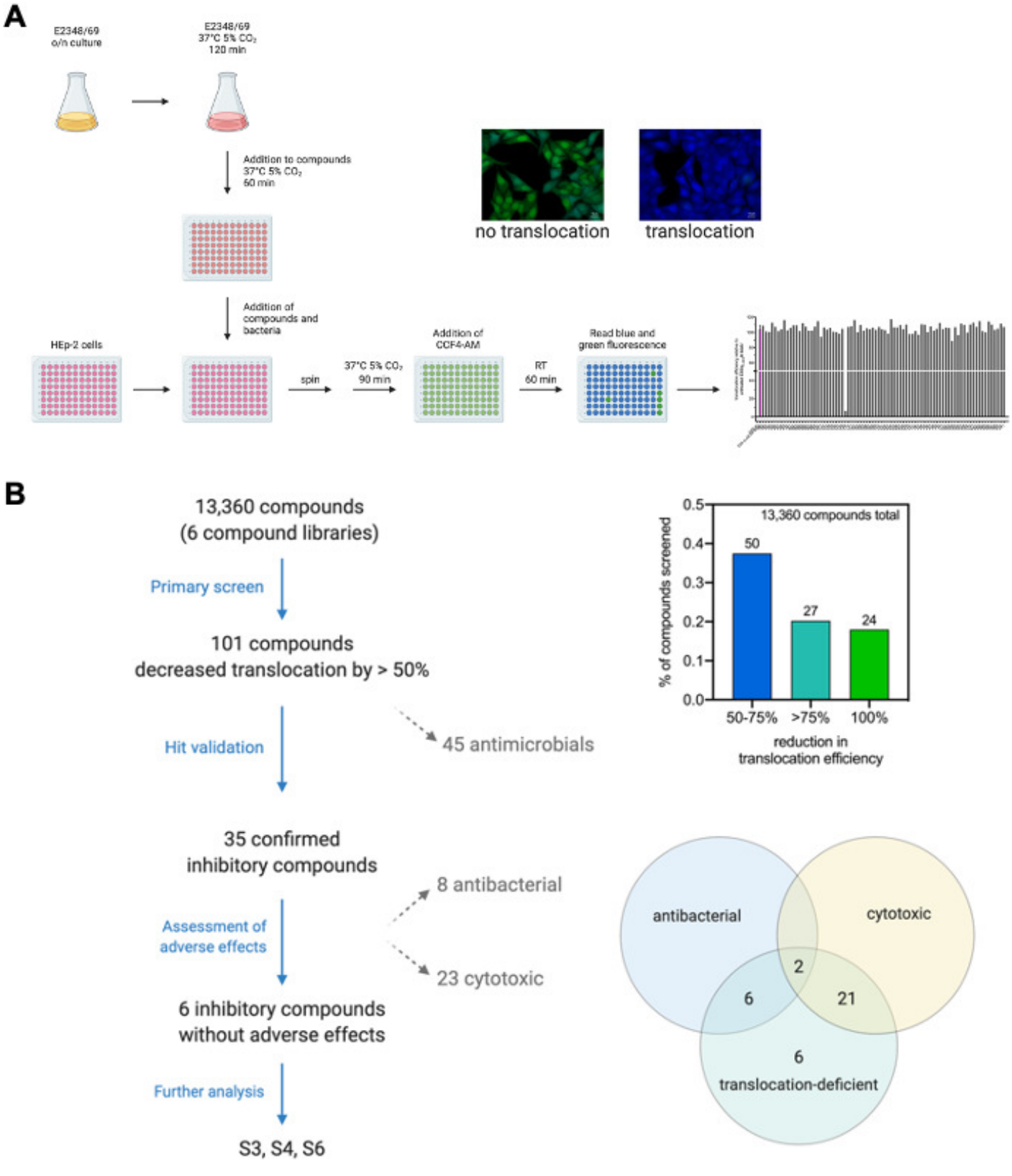

FIG 1 Mühlen *et al.* 2021

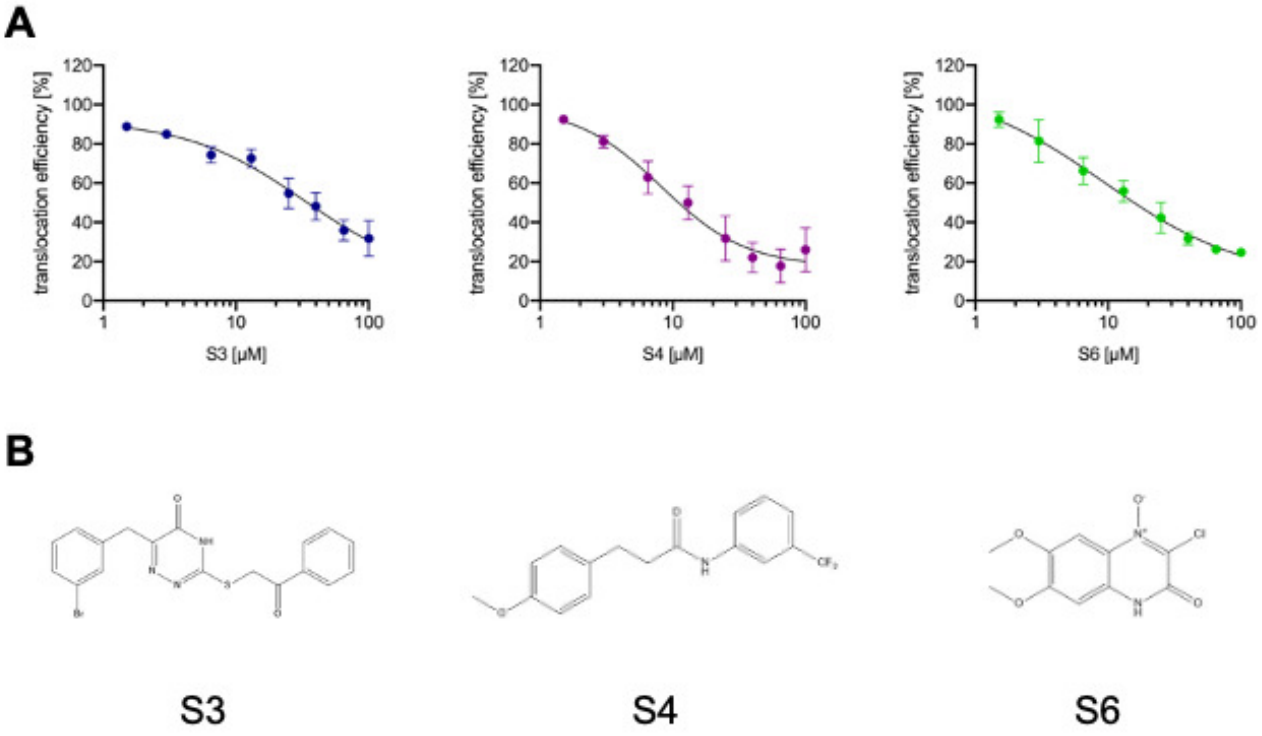

FIG 2 Mühlen *et al.* 2021

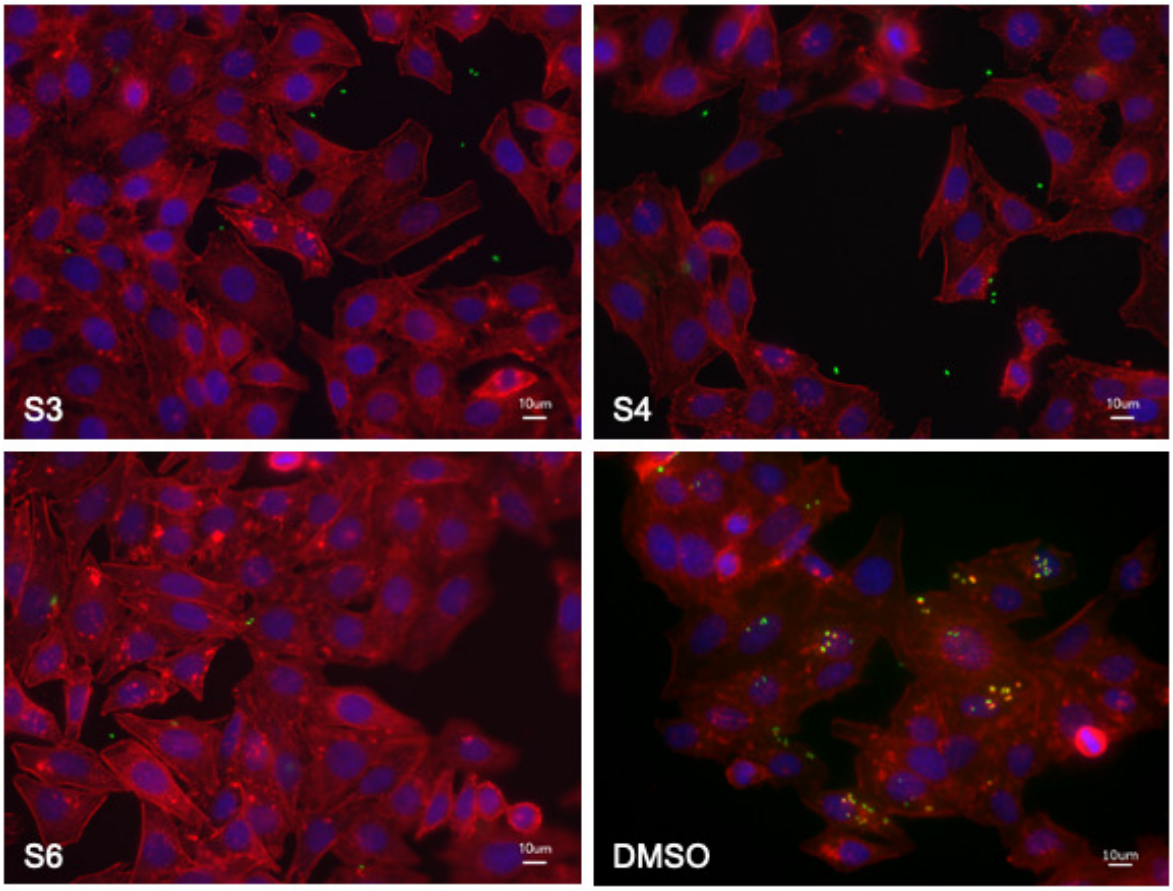

FIG 3 Mühlen *et al.* 2021

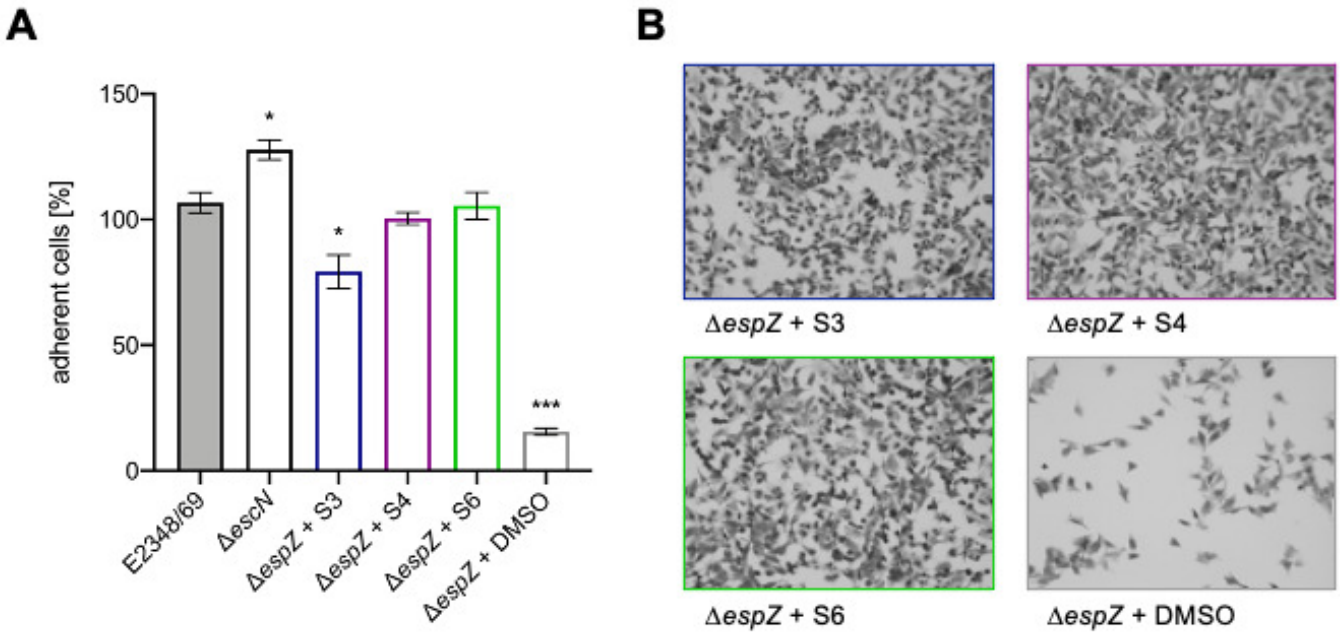

FIG 4 Mühlen *et al.* 2021

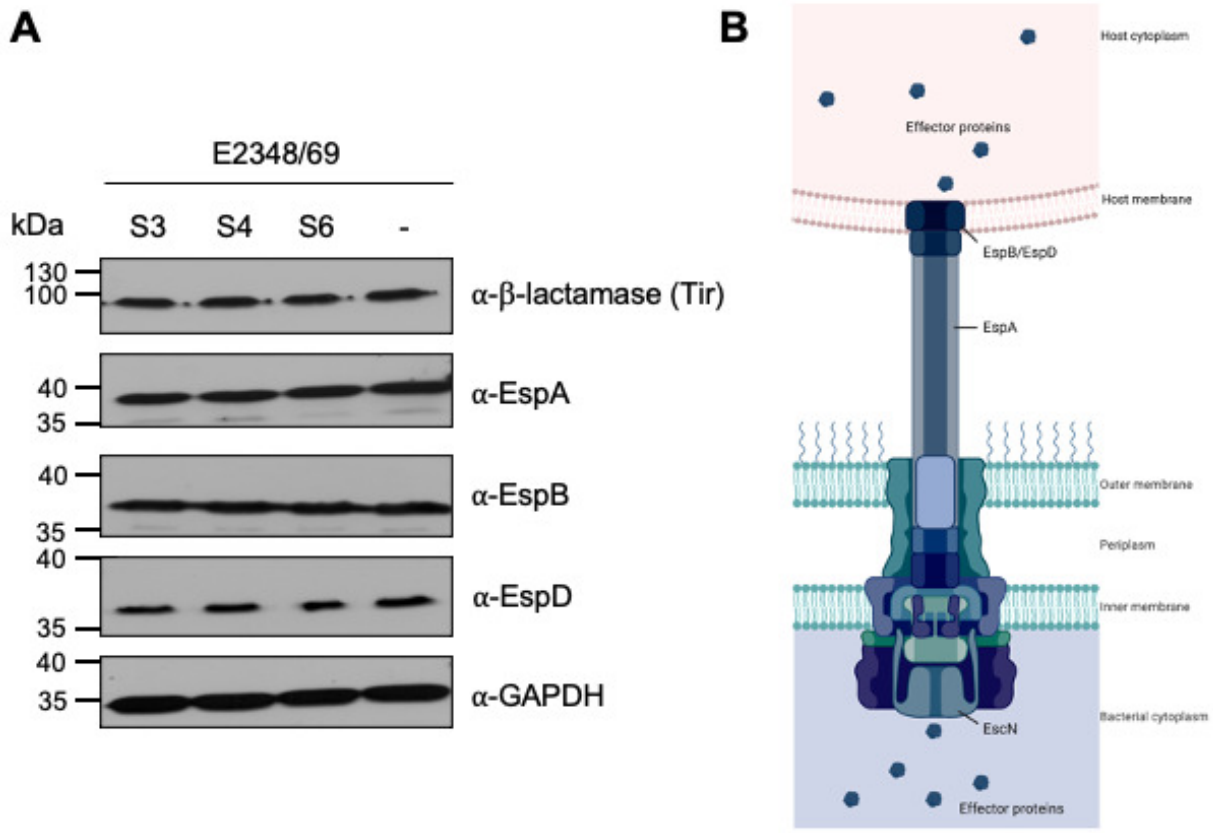

FIG 5 Mühlen *et al.* 2021

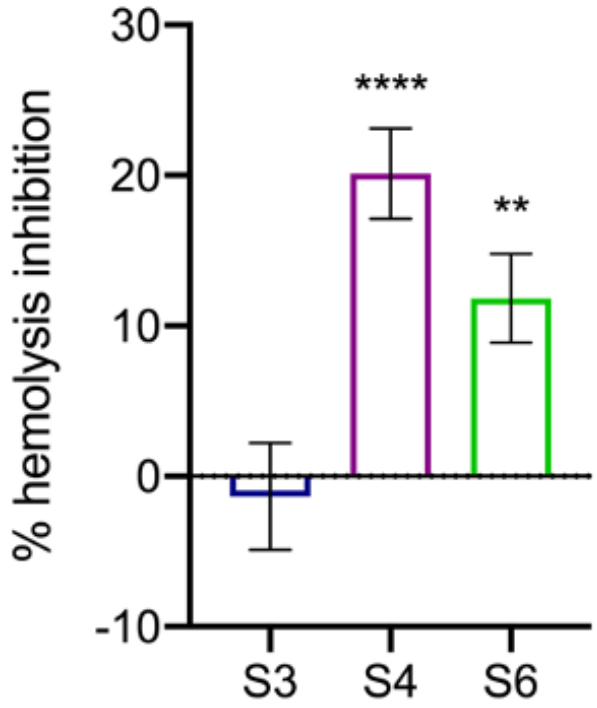

FIG 6 Mühlen *et al.* 2021

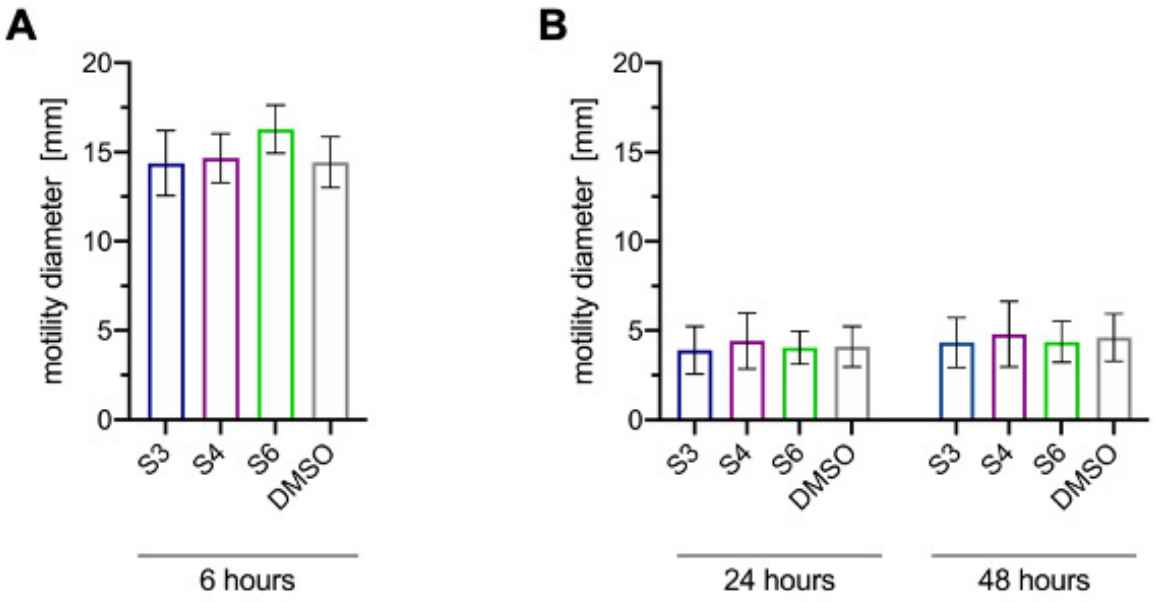

FIG 7 Mühlen *et al.* 2021

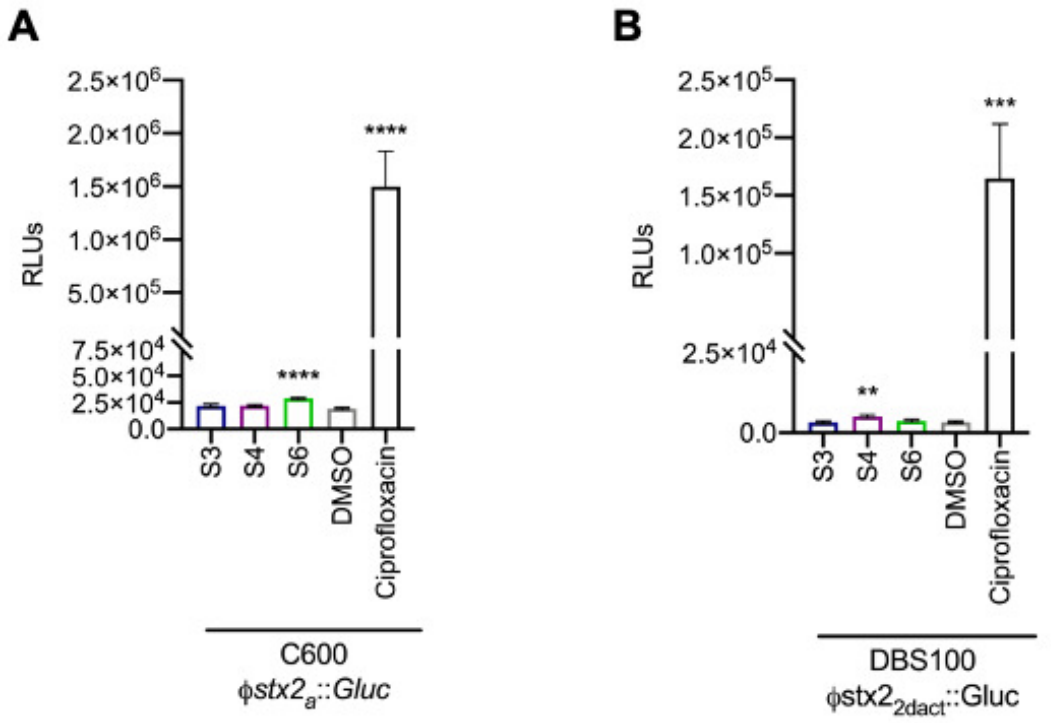

FIG 8 Mühlen *et al.* 2021